European Journal of Nuclear Medicine and Molecular Imaging (2021) 48:1550–1559
https://doi.org/10.1007/s00259-020-05081-6

ORIGINAL ARTICLE

Physiologic colonic uptake of ^{18}F-FDG on PET/CT is associated with clinical response and gut microbiome composition in patients with advanced non-small cell lung cancer treated with immune checkpoint inhibitors

Lena Cvetkovic[1,2] · Claudine Régis[3,4] · Corentin Richard[2] · Lisa Derosa[5] · Antoine Leblond[3,6] · Julie Malo[1,2] · Meriem Messaoudene[1,2] · Antoine Desilets[1,2] · Wiam Belkaid[1,2] · Arielle Elkrief[1,2] · Bertrand Routy[1,2] · Daniel Juneau[2,3,7]

Received: 15 August 2020 / Accepted: 15 October 2020 / Published online: 31 October 2020

Abstract

Background Immune checkpoint inhibitors (ICI) represent the backbone treatment for advanced non-small cell lung cancer (NSCLC). Emerging data suggest that increased gut microbiome diversity is associated with favorable response to ICI and that antibiotic-induced dysbiosis is associated with deleterious outcomes. ^{18}F-FDG physiologic colonic uptake on PET/CT increases following treatment with antibiotics (ATB) and could act as a surrogate marker for microbiome composition and predict prognosis. The aim of this study was to determine if ^{18}F-FDG physiologic colonic uptake prior to ICI initiation correlates with gut microbiome profiling and clinical outcomes in patients with advanced NSCLC.

Methods Seventy-one patients with advanced NSCLC who underwent a PET/CT prior to ICI were identified. Blinded colonic contouring was performed for each colon segment and patients were stratified according to the median of the average colon SUV_{max} as well as for each segment in low vs. high SUV_{max} groups. Response rate, progression-free survival (PFS), and overall survival (OS) were compared in the low vs. high SUV_{max} groups. Gut microbiome composition was analyzed for 23 patients using metagenomics sequencing.

Results The high colon SUV_{max} group had a higher proportion of non-responders ($p = 0.033$) and significantly shorter PFS (4.1 vs. 11.3 months, HR 1.94, 95% CI 1.11–3.41, $p = 0.005$). High caecum SUV_{max} correlated with numerically shorter OS (10.8 vs. 27.6 months, HR 1.85, 95% CI 0.97–3.53, $p = 0.058$). Metagenomics sequencing revealed distinctive microbiome populations in each group. Patients with low caecum SUV_{max} had higher microbiome diversity ($p = 0.046$) and were enriched with *Bifidobacteriaceae*, *Lachnospiraceae*, and *Bacteroidaceae*.

Lena Cvetkovic and Claudine Régis contributed equally to this work.

This article is part of the Topical Collection on Oncology - Chest.

Supplementary Information The online version contains supplementary material available at https://doi.org/10.1007/s00259-020-05081-6.

✉ Bertrand Routy
bertrand.routy@umontreal.ca

✉ Daniel Juneau
daniel.juneau@umontreal.ca

[1] Department of Hematology and Oncology, Centre hospitalier de l'Université de Montréal (CHUM), Montréal, Québec, Canada

[2] Centre de recherche du Centre hospitalier de l'Université de Montréal (CRCHUM), Université de Montréal, Montréal, Québec, Canada

[3] Department of Radiology and Nuclear Medicine, Centre hospitalier de l'Université de Montréal (CHUM), Montréal, Québec, Canada

[4] Department of Radiology and Nuclear Medicine, Institut de Cardiologie de Montréal, Montréal, Québec, Canada

[5] Department of Tumor Immunology and Immunotherapy INSERM U1015, Gustave Roussy Cancer Center, Villejuif, France

[6] Department of Radiology and Nuclear Medicine, Centre Hospitalier Affilié Universitaire Régional (CHAUR), Trois-Rivières, Québec, Canada

[7] University of Ottawa Heart Institute, Ottawa, Ontario, Canada

Conclusions Lower colon physiologic ^{18}F-FDG uptake on PET/CT prior to ICI initiation was associated with better clinical outcomes and higher gut microbiome diversity in patients with advanced NSCLC. Here, we propose that ^{18}F-FDG physiologic colonic uptake on PET/CT could serve as a potential novel marker of gut microbiome composition and may predict clinical outcomes in this population.

Keywords ^{18}F-FDG colonic uptake · Gut microbiome · Non-small cell lung cancer · Immunotherapy · Metagenomics

Background

Immune checkpoint inhibitors (ICI) now represent the therapeutic backbone for patients with advanced non-small cell lung cancer (NSCLC). Landmark trials first compared PD-1/PD-L1 inhibitors to standard chemotherapy in previously treated metastatic NSCLC and demonstrated superior overall survival (OS) in the ICI groups with a sustained response in 20% of patients at 4 years [1–5]. These results led to the study of ICI in first-line settings, with unprecedented improvements in OS with either single-agent anti-PD-1 [6] or in combination with chemotherapy [7] leading to implementation of these treatments as the standard-of-care [8].

Despite these positive results, primary resistance rates of 47–63% remain the major therapeutic hurdle [9–11], and existing biomarkers of response including PD-L1 expression and tumor mutational burden are unable to consistently and accurately predict response to ICI [12]. Addressing these unmet needs, the gut microbiome has emerged as a potential biomarker of response to ICI with a scope across a wide array of immunogenic malignancies including advanced NSCLC [13]. Indeed, several studies have demonstrated the association between high baseline bacteria diversity as a positive predictor of response across a myriad of cancers. In addition, specific gut microbial bacteria have been associated with response to ICI in NSCLC [13–17], as well as melanoma and renal cell carcinoma (RCC). Furthermore, the use of antibiotics (ATB) prior to the initiation of ICI has been associated with worse clinical outcomes in more than 2300 patients receiving ICI [18–21]. Two recent studies indicated that in patients with RCC and NSCLC, ATB prior to ICI initiation decreases gut microbial diversity as well as increases specific deleterious bacteria such as *Clostridium hathewayi* [22, 23].

However, there is currently a paucity of easily accessible and routinely performed clinical tools to accurately collect and define gut microbiome composition. 2-deoxy-2-[fluorine-18]-fluoro-D-glucose (^{18}F-FDG) positron emission tomography combined with computed tomography (PET/CT) is a marker of tissue glucose metabolism and is routinely used to stage and to assess therapeutic response in NSCLC [8]. Due to the gut microbiota's metabolism of glucose [24], it was hypothesized that ^{18}F-FDG colon uptake on PET/CT could describe shifts in the microbiota composition after ATB use in patients [25]. Indeed, Boursi et al. showed that patients who received ATB had a higher physiologic colon uptake potentially correlating with decreased bacterial diversity compared to patients who did not receive ATB. Therefore, we sought to determine whether ^{18}F-FDG PET/CT could serve as a novel, non-invasive tool to assess gut microbiome composition and as a prognostic biomarker in patients with advanced NSCLC treated with ICI.

Methods

Study population

We retrospectively identified 71 patients at the Centre hospitalier de l'Université de Montréal (CHUM) with advanced NSCLC who underwent a ^{18}F-FDG PET/CT prior to ICI. Inclusion criteria for the study were patients with advanced NSCLC (stage IV or those with unresectable or recurrent disease not amenable to definitive treatment), treated with anti-PD-1/PD-L1 monotherapy or in combination with chemotherapy at recommended dose either as first-line or later-line therapy, between December 2015 and September 2019. Patients who had received ATB 2 months prior to ICI were excluded. Patients on metformin were also excluded, since this can impact the uptake of ^{18}F-FDG in the colon [26]. Fecal samples were available for 23 patients that are included in a separate ongoing prospective biobank of NSCLC patients amenable to immunotherapy. All clinical data were extracted through the CHUM's electronic medical records. The study protocol was approved by the local Ethics Committee "Comité d'éthique de la recherche du CHUM" (Ethics number CER CHUM: 18.039 and 18.085-17.035) and conducted in accordance with the tenets of the Declaration of Helsinki. The need for informed patient consent was waived.

PET/CT imaging protocol

Patients were required to be fasting at least 4 h prior to FDG injection. Blood sugar below 11.0 mmol/L was required for all patients. A total of 3.5 MBq/kg of ^{18}F-FDG was injected intravenously, followed by standard whole-body PET/CT scan at 60-90 min post-injection. Images were obtained with either a GE Discovery IQ (GE Healthcare, Milwaukee, USA) or a Siemens Biograph mCT (Siemens Healthcare, Erlangen,

Germany). CT without intravenous contrast was used for attenuation correction and localization and CT acquisitions' parameters were 120 kV, 10-20 mA, 0.5–0.8 s per rotation, and 3.0–3.75 mm slice thickness.

PET/CT image analysis

For each patient, colonic segmentation and contouring were performed by a single nuclear medicine physician blinded to all clinical information. To perform the segmentation, the colon was divided in its five anatomic segments (caecum, right, transverse, left, and rectosigmoid) and contouring of each portion was performed separately.

Contouring was performed by manually drawing regions of interest (ROI) surrounding the colon on axial CT images, which were then transposed automatically onto the corresponding axial PET-AC images. Coregistration of PET and CT images was reviewed for each study visually by the nuclear medicine physician. For the first 10 patients analyzed, we compared two distinct techniques. In the first technique, every single axial slice containing the colon was contoured, while in the second technique, only 1 out of 4 consecutive axial slices was contoured. We analyzed the agreement between the two methods using Bland-Altman plots and found excellent agreement. Based on this, the second technique was used for all patients. A representative sample of a colonic segmentation is presented in Fig. 1. After contouring, the SUV_{max} of each ROI were recorded. An average SUV_{max} was calculated for the whole colon and for each segment. Patients were stratified in two groups according to the median of the average colon SUV_{max}: low vs. high uptake groups. Patients were also stratified in groups according to the median SUV_{max} of each individual segment.^{18}F-FDG uptake for the entire colon and each segment was then compared to response rate, progression-free survival (PFS), and overall survival (OS).

Metagenomic analysis of patient fecal samples

Fecal samples were collected by patients at home and conserved at 5 °C, then frozen 4-24 h later at − 80 °C according to International Human Microbiome Standard guideline [27]. Twenty-three patients had available fecal samples at baseline and 3 patients were collected for a second sample after 2 cycles of ICI.

Total fecal DNA was extracted as described previously by Suau et al. [28] and sequenced using ion-proton technology (Thermo Fisher) resulting in 22.7 ± 0.9 million (mean ± SD) single-end short reads of 150-base-long single-end reads as a mean. Single-end reads were processed using the YAMP pipeline, v0.9.4.3 [29]. In the QC step, identical reads, adapters, known artifacts, and phix174 were removed. Reads were quality trimmed (PhRED quality score < 10) and resulting reads that became too short after trimming (N < 60 bp) were discarded. Then, contaminant reads belonging to the host genome were removed (build: GRCh37). We obtained an average number of reads of 20.8 million per sample. Finally, YAMP was used to characterize the microbial community (via MetaPhlAn2, v. 2.6.0 [30]).

Downstream analyses were performed at the species level through the R software v4.0.0 and phyloseq R package v1.30.0 [31]. The alpha-diversity was calculated as number of observed species. Mann-Whitney U test was used to compare groups according to this value. Bray–Curtis distance [32] was used as beta-diversity metrics and visualized through NMDS (non-metric multidimensional scaling) method [33]. PERMANOVA test was used to compare groups according to Bray-Curtis distance. DESeq2 [34] was used to perform differential abundance analysis at the genus level. The p values were corrected with the Benjamin-Hochberg procedure for the DESeq2 differential abundance analysis.

Statistical analysis

Statistical analysis was performed using the GraphPad Prism software (v7, GraphPad Software, San Diego, USA). Clinical endpoints were response rate and survival. Objective response was defined by the rate of complete response (CR) and partial response (PR). Responder status was defined by proportion of patients with CR + PR + stable disease (SD) > 6 months. We also measured the rate of progression of disease (PD). Survival was assessed with PFS (defined by time of first injection of ICI to the first event (tumor progression or death from any cause)) and OS (defined by time of first injection of ICI to the date of death from any cause). Patient outcomes were reported using RECIST1.1 criteria [35]. Patients with no events were censored at the date of last follow-up. Fisher's exact test was used to analyze response rate. Survival curves were estimated through the Kaplan-Meier method and compared with the log-rank test [36, 37]. T test was used to determine the difference in SUV_{max} between the high and low SUV_{max} groups for each segment of the colon. Statistical significance was defined as p value < 0.05.

Results

Patient population and segregation of patients into high and low colon SUV_{max}

Seventy-one patients with advanced NSCLC treated with anti-PD-1, either as monotherapy or in combination with chemotherapy, were included in this study with a median follow-up of 17.9 months. Baseline characteristics of all patients are presented in Supplemental Table 1. Median age was 68 years and 33 (46%) patients were female. Sixty patients (85%) had

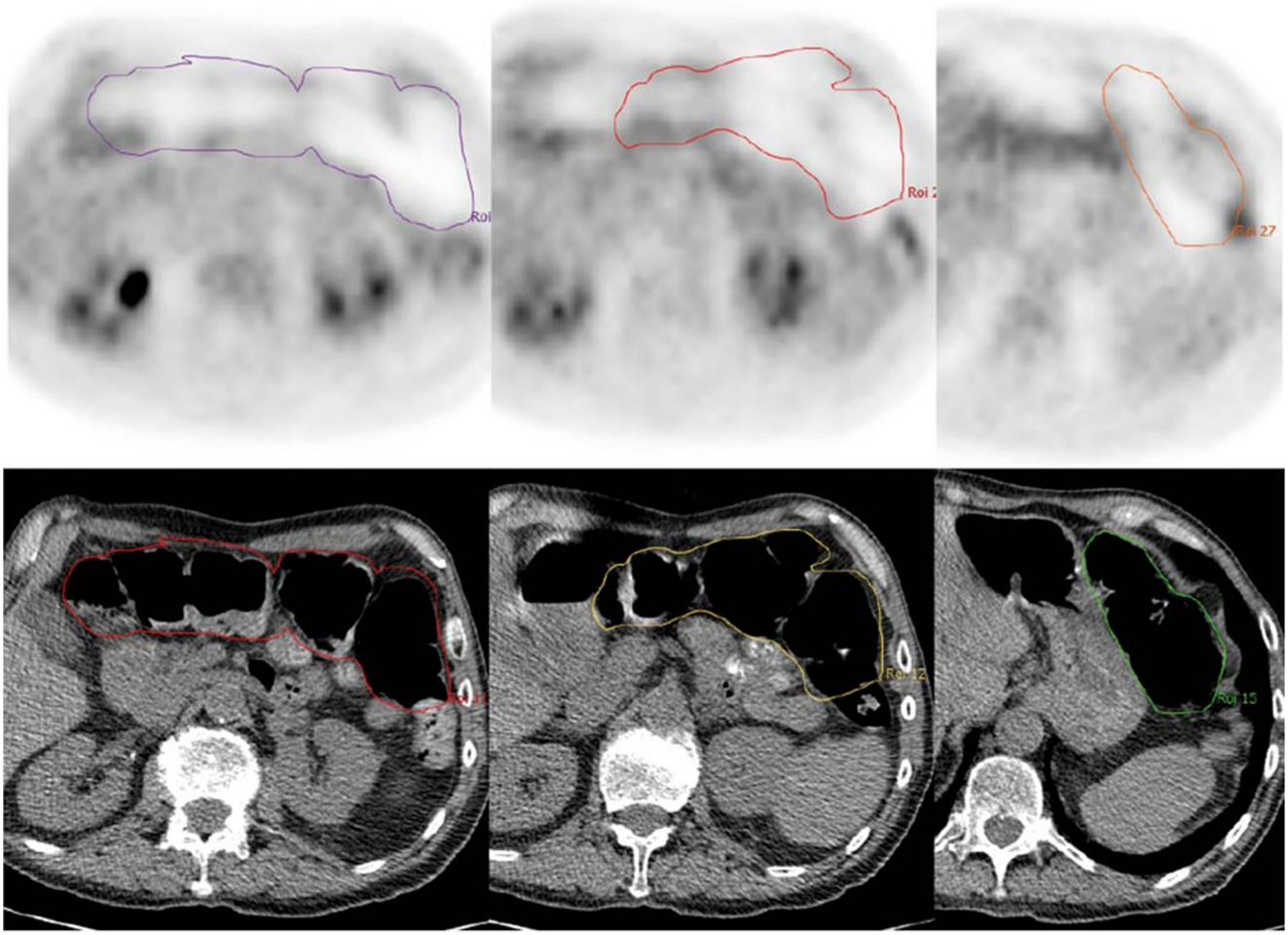

Fig. 1 Representative example of colonic segmentation and contouring on PET/CT

stage IV disease. Forty-four patients (62%) had chemotherapy-refractory disease and were treated with anti-PD-1 monotherapy in the second-line setting, while 27 patients (38%) were treated with first-line anti-PD-1. Eight patients (11%) received anti-PD-1 in combination with chemotherapy.

As described in the methods, after contouring of the colon (Fig. 1), patients were divided into two groups based on the median of the average colon SUV_{max}: low colon SUV_{max} (below the median) and high colon SUV_{max} (above the median) groups. The average colon SUV_{max} for the low SUV_{max} and high SUV_{max} groups were 1.41 (95% CI 1.35–1.47) and 2.18 (95% CI 1.90–2.46) respectively. Representative physiologic colonic uptake is presented in one patient from the low colon SUV_{max} and one patient from the high colon SUV_{max} group in Fig. 2. Baseline characteristics were well balanced between the two SUV_{max} groups with no significant differences with respect to sex, ECOG performance status, lung cancer histology, lung cancer stage, PD-L-1 expression, type of anti-PD-1 monoclonal antibody, and line of ICI (Supplemental Table 1).

Individual colon segment SUV_{max} analysis

The SUV_{max} of each segment for the low colon SUV_{max} group was compared to the respective segment of the high colon SUV_{max} group. There was a significant difference between the low colon SUV_{max} and the high colon SUV_{max} for each of the five segments of the colon ($p = 0.001$) respectively (Fig. 3). Interestingly, we identified that the SUV_{max} in the left colon and transverse colon were significantly lower than the three other segments, namely caecum, right colon, and rectosigmoid ($p < 0.001$). Altogether, these results demonstrated that the average colon SUV_{max} was homogeneously distributed throughout the entire colon.

Whole colon ^{18}F-FDG uptake vs. clinical outcome

We compared the response rates for the patients in each colon SUV_{max} group. In the low colon SUV_{max} group, 11.4%, 17.1%, 34.3%, and 37.2% patients achieved CR, PR, SD,

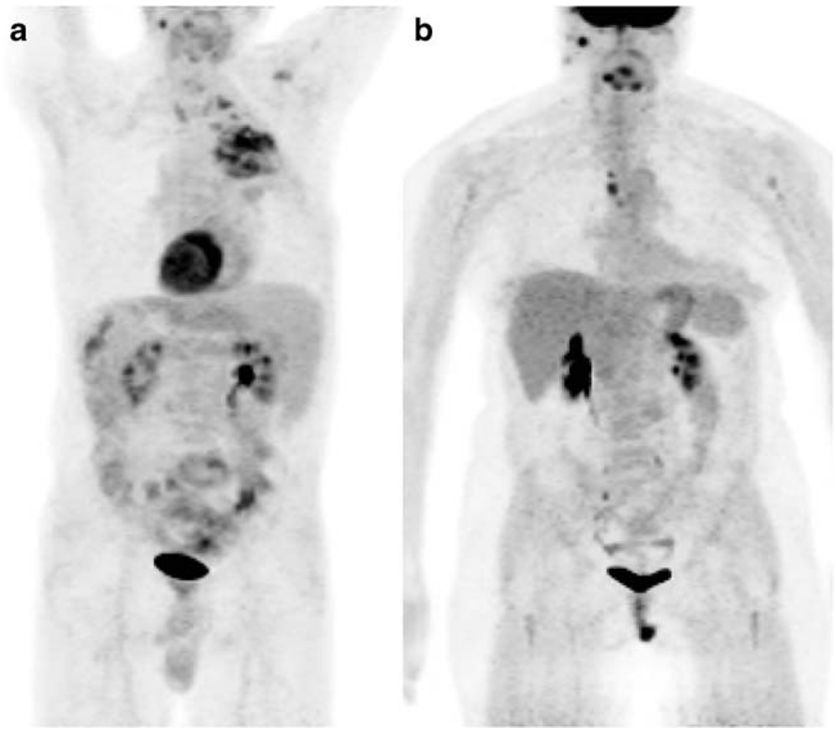

Fig. 2 **a** Maximum intensity projection (MIP) of the ^{18}F-FDG PET study of a representative patient from the high colon SUV_{max} group with a mean colon SUV_{max} of 2.6, and from a patient from the low colon SUV_{max} group **b** with a mean colon SUV_{max} of 1.3

and PD respectively. In the high colon SUV_{max} group, 17.5%, 17.5%, and 65% patients achieved PR, SD, and PD respectively. No patient achieved CR in the high colon SUV_{max} group. The high colon SUV_{max} group had a higher proportion of patients with progressive disease ($n = 22$, 65%) compared to the low colon SUV_{max} group ($n = 13$, 37.2%) ($p = 0.033$) (Fig. 4a). In addition, patients in the high colon SUV_{max} group had a significantly shorter PFS of 4.1 months vs. 11.3 months in the low SUV_{max} group (HR 1.94, 95% CI 1.11–3.41) ($p = 0.005$) (Fig. 4b). When comparing the high colon SUV_{max} group to the low colon SUV_{max} group, there was no difference in OS.

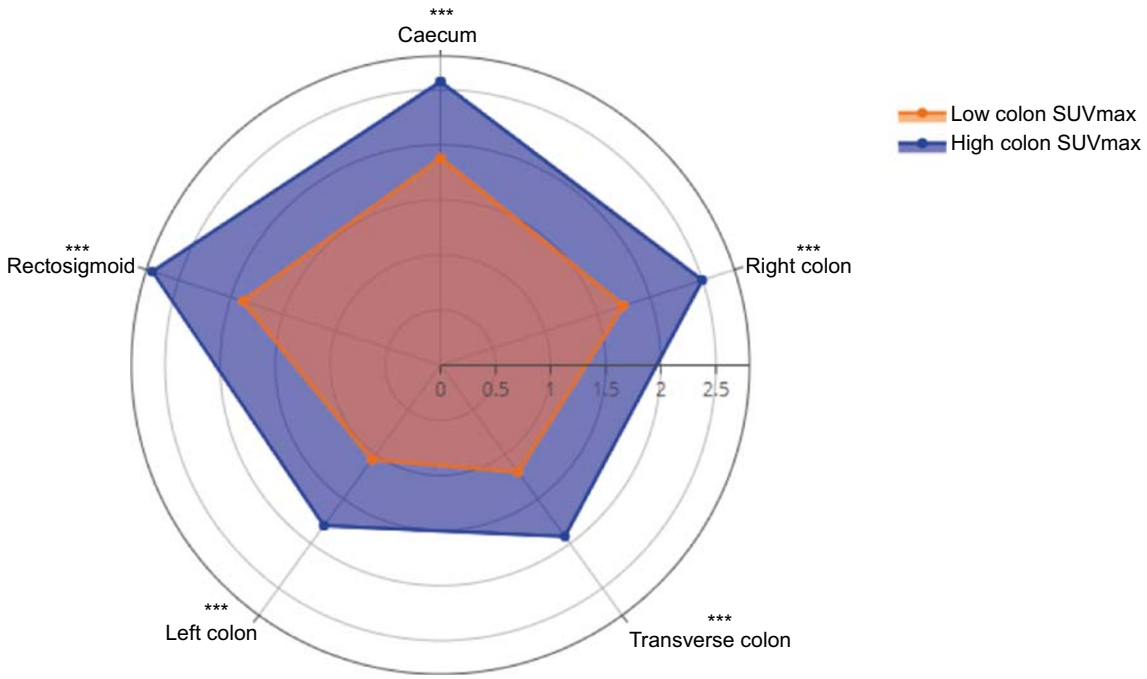

Fig. 3 Radar plot showing the differences in SUV_{max} throughout the segments of the colon between the low colon SUV_{max} and the high colon SUV_{max} groups. ***$p = 0.001$

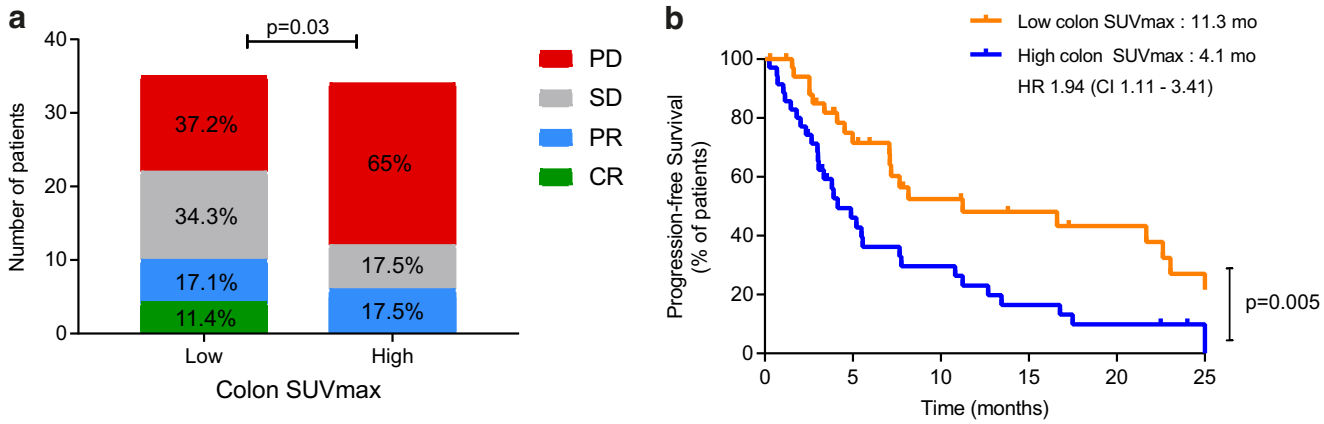

Fig. 4 **a** Response rates for patients with low colon SUV_{max} compared to those with high colon SUV_{max}. PD: progressive disease; SD: stable disease; PR: partial response; CR: complete response**.** Percentage (%) represents the proportion of patients in each group that achieved each response. $p = 0.03$. **b** Progression-free survival for patients with low colon SUV_{max} compared to those with high SUV_{max}. $p = 0.005$. Mo: months

Colonic segment ^{18}F-FDG uptake vs. clinical outcome

Each of the 5 segments were also analyzed individually with respect to clinical outcome. The average caecum SUV_{max} for the low and high caecum uptake groups were 1.61 (95% CI 1.49–1.73) and 2.82 (95% CI 2.61–3.02) respectively. When evaluating response rate, the high caecum SUV_{max} group had a higher proportion of patients with progressive ($n = 23$, 67.6%) disease compared to low caecum SUV_{max} group ($n = 13$, 34.3%) ($p = 0.03$) (Fig. 5a). Furthermore, we found that patients in the high caecum SUV_{max} group had a significantly shorter PFS compared to the low caecum SUV_{max} group (4.1 months vs. 8.2 months, HR 1.97, 95% CI 1.14–3.39) ($p = 0.01$) (Fig. 5c) and an important numerical disadvantage in OS (10.8 months vs. 27.8 months, HR 1.97, 95% CI 1.14–3.39) ($p = 0.058$) (Fig. 5b). None of the analysis for the right, transverse, left, and rectosigmoid colon reached statistical significance.

Metagenomics sequencing of fecal sample analysis

Metagenomics sequencing on available fecal samples ($n = 23$) was performed in an attempt to link SUV_{max} to gut microbiome diversity and composition. Alpha-diversity analysis—which represents the number of bacteria in each sample—showed higher microbiome diversity in patients with low caecum SUV_{max} ($p = 0.046$) (Fig. 6a). Beta-diversity analysis showed that patients with low caecum SUV_{max} and patients with high caecum SUV_{max} had a significant difference in the global composition of their microbiome ($p = 0.04$) (Fig. 6b).

Finally, differential abundance analysis using DESeq2 algorithm revealed that patients with low caecum SUV_{max} were enriched with bacteria species of *Bifidobacteriaceae*, *Lachnospiraceae*, and *Bacteroidaceae* families compared to high caecum SUV_{max} (Fig. 6c).

Discussion

In this study in patients with advanced NSCLC who underwent ^{18}F-FDG PET/CT prior to ICI, those in the high colon SUV_{max} group had a higher proportion of non-responders ($p = 0.033$), and significant shorter PFS (4.1 months vs. 11.3 months, $p = 0.005$) and no difference in

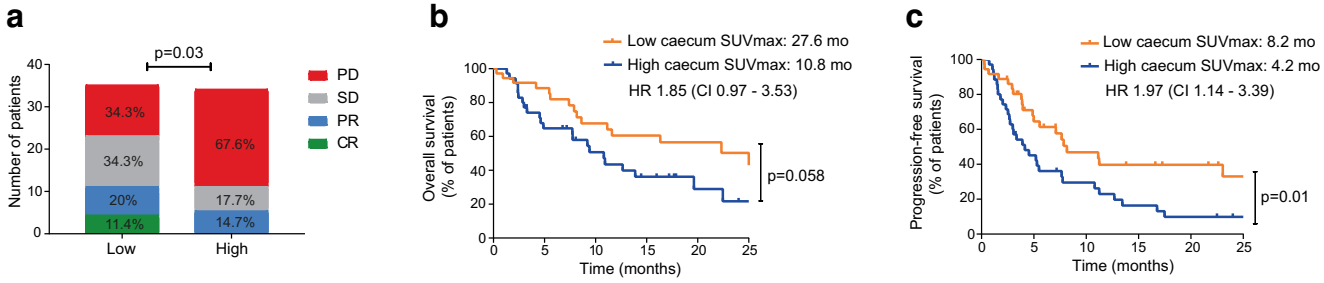

Fig. 5 **a** Response rates for patients with low caecum SUV_{max} compared to those with high caecum SUV_{max}. PD: progressive disease; SD: stable disease; PR: partial response; CR: complete response**.** Percentage (%) represents the proportion of patients in each group that achieved each response. $p = 0.03$. **b** Overall survival for patients with low caecum SUV_{max} compared to those with high caecum SUV_{max}. $p = 0.058$. Mo: months. **c** Progression-free survival for patients with low caecum SUV_{max} compared to those with high caecum SUV_{max}. $p = 0.01$. Mo: months

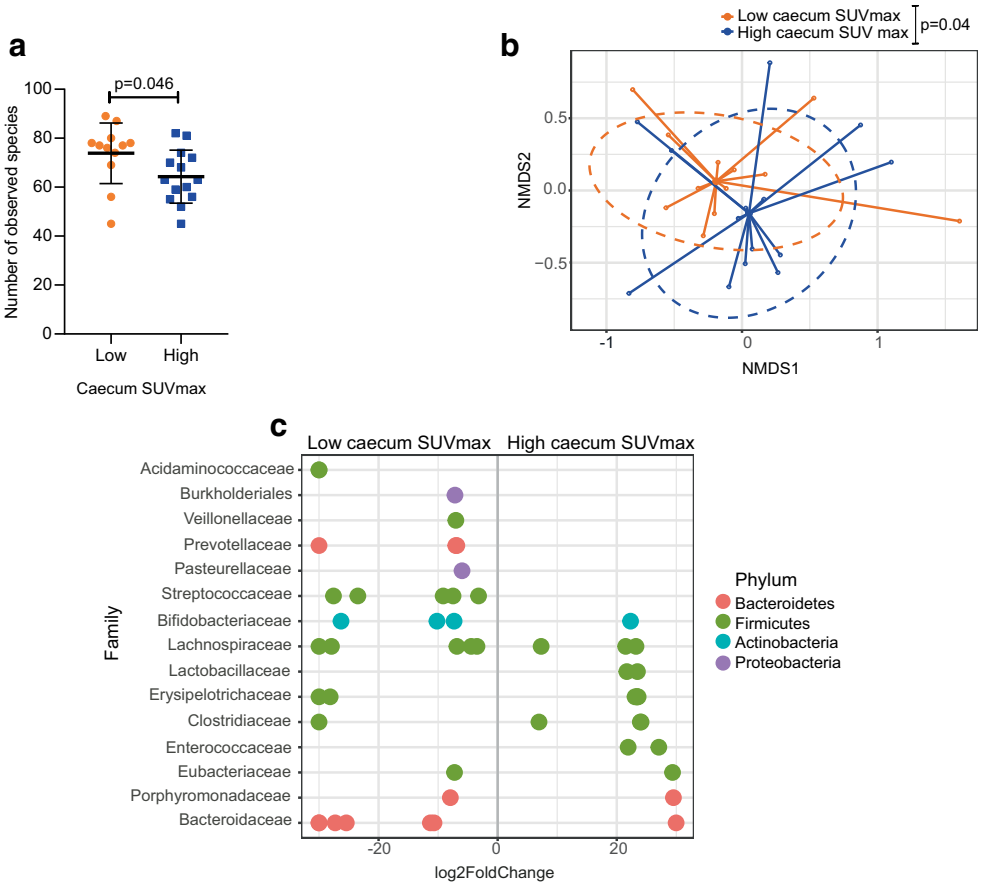

Fig. 6 **a** Alpha-diversity analysis by number of observed species for patients with low caecum SUV_{max} compared with high caecum SUV_{max}. $p = 0.046$. **b** Beta-diversity analysis by Bray-Curtis distance, showing two distinctive microbiome composition between the low caecum SUV_{max} and the high caecum SUV_{max} groups. $p = 0.04$, NMDS: non-metric multidimensional scaling. **c** DESeq2 analysis depicting differential abundance of bacteria in caecum SUV_{max} in low vs. high groups

OS. Sub-analysis of the colon segments was performed, and the patients in the high caecum SUV_{max} group also trended towards a shorter OS (10.8 vs. 27.6 months, $p = 0.058$) compared to low caecum SUV_{max} group. Subsequently, gut microbiome metagenomics showed a higher microbial alpha-diversity amongst the low caecum SUV_{max} group. Beta-diversity analysis showed different bacterial species, with segregation of two distinct bacterial clusters in the two SUV_{max} groups. Finally, specific beneficial bacteria were enriched in the low SUV_{max} group such as *Bifidobacteriaceae*, *Lachnospiraceae*, and *Bacteroidaceae*.

To our knowledge, this is the first study demonstrating a correlation between physiologic colon SUV_{max} and response to ICI in patients with advanced NSCLC treated with ICI. Furthermore, we demonstrated an association between the SUV_{max} in the colon and the gut microbiome diversity. Altogether, these results demonstrate the potential use of ^{18}F-FDG PET/CT as a novel and non-invasive tool to determine gut microbial composition. This could be potentially explained by a correlation between low bacterial diversity and gut immune inflammation associated with high SUV_{max}. Indeed, patients with obesity and inflammatory bowel disease have been shown to have lower gut microbial diversities compared to healthy individuals, and this low diversity is associated with local and systemic inflammation [38–40]. Further linking PET/CT colonic uptake with the gut microbiome, a previous study by Boursi et al. examined the use of ^{18}F-FDG PET/CT to further characterize the complex relationship between the gut microbiota and colon ^{18}F-FDG PET/CT. In this prospective study, they enrolled healthy volunteers who underwent ^{18}F-FDG PET/CT and performed gut microbial sampling before and after ATB use. Using similar contouring methods as described in our paper, the authors found a significant increase in physiologic ^{18}F-FDG colon uptake, with a mean increase in SUV_{max} of 0.63 ± 0.37 SD ($p = 0.004$) post ATB treatment. Boursi et al. also conducted a retrospective study addressing the role of ^{18}F-FDG PET/CT as a biomarker of response in patients with metastatic melanoma. In this study of 14 patients with metastatic melanoma treated with ICI, the patients with complete response (CR) had a lower colonic mean SUV_{max} compared to those without CR (partial response or disease progression) ($p = 0.03$) [41].

Recently, gut microbiome diversity has emerged as a promising biomarker to predict response to ICI in cancer patients [13, 16, 22]. Several papers have unraveled that ICI efficacy correlated with high baseline diversity and specific immune potentiating gut microbiome bacteria. Indeed, in several cohorts of patients with NSCLC, melanoma, and RCC treated with ICI,

low baseline microbiota diversity defined by alpha indexes correlated with poor outcome [13, 22]. These pre-clinical experiments in germ-free or ATB-treated mice illustrate the need for an intact microbiome [13]. Multiple observational studies demonstrated that ATB use pre-ICI initiation led to a significant decrease in outcomes. Recently, two papers identified that ATB had a direct impact on microbiome diversity and ATB use pre-ICI led to a decrease in microbiome diversity [22, 23].

Furthermore, gut microbiome bacteria such as *Bifidobacterium*, *Agathobacter* member of *Lachnospiraceae*, *Bacteroides fragilis* member of *Bacteroidaceae*, and *Akkermansia muciniphila* were enriched in patients with favorable outcome [13, 42]. Surrogate markers of immune activation such as $CD8^+$ and low Treg also positively correlated with the abundances of these bacteria [15, 16]. Interestingly, beyond the correlation between diversity and SUV_{max}, at the taxonomic level, we found that *Bifidobacteriaceae*, *Lachnospiraceae*, and *Bacteroidaceae* were enriched in patients with low caecum SUV_{max} and therefore associated with better survival. These findings are consistent with previous papers by Matson et al., Hakozaki et al., and Vétizou et al. that described a higher proportion of *Bifidobacterium*, *Agathobacter*, and *Bacteroides fragilis* in patients that had a good response to ICI [16, 17, 43]. Beyond biomarker studies, clinical trials evaluating combination oral supplementation of *Bifidobacterium* probiotics with ICI are currently underway (NCT03817125, NCT03775850).

Despite being the largest study to date demonstrating the potential role of ^{18}F-FDG PET/CT as a non-invasive biomarker linking colonic uptake of ^{18}F-FDG to clinical outcomes and microbiome diversity using metagenomics, our study has several limitations. Firstly, this was a single-center retrospective study. Therefore, external validation using different software and hardware might be warranted before this technique can be applied more widely. Furthermore, our study had a relatively low sample size, which could explain why the difference in OS between the high and low SUV_{max} groups did not reach statistical significance. Also, fecal samples were not available for all the patients included in the study. Despite this, we were still able to find a statistically significant correlation between low caecum SUV_{max} and higher microbiome diversity. Finally, while the current segmentation technique is operator-dependant and time-intensive, with the significant advances that have been achieved in machine-learning and automated segmentation over the last few years, it is only a question of time before it can be simplified and applied in a clinical setting.

Conclusion

In our study of 71 patients with advanced NSCLC treated with ICI, lower colon SUV_{max} on ^{18}F-FDG PET/CT is associated with better clinical outcomes and higher baseline gut microbiome diversity and specific differentially abundant commensals. ^{18}F-FDG physiologic colonic uptake on PET/CT has the potential to become a novel marker of gut microbiome composition and might predict clinical outcomes in this population. Future prospective trials are needed in order to determine whether this tool could serve as a surrogate marker of gut microbiome composition in order to predict clinical outcomes in patients being considered for ICI treatment.

Author contributions Bertrand Routy and Daniel Juneau have conceptualized the study and contributed to drafting of the original manuscript. Bertrand Routy, Daniel Juneau, and Arielle Elkrief contributed to supervision. Lena Cvetkovic, Claudine Régis, and Arielle Elkrief were responsible for data acquisition and analysis as well as original manuscript preparation. Corentin Richard, Lisa Derosa, Antoine Leblond, Julie Malo, Meriem Messaoudene, Antoine Desilets, and Wiam Belkaid have acquired and analyzed data and contributed to drafting the manuscript. All authors have contributed substantially to the final work and agree on its contents.

Funding B. Routy was supported by H2020 ONCOMICROBIOME. L. Derosa's salary was supported by the RHU Torino Lumière (ANR-16-RHUS-0008).

Compliance with ethical standards

Conflict of interest DJ has received consultant fees from AbbVie and Advanced Accelerator Applications. BR reports acting as a Scientific Advisory Board Member for Vedanta. All other authors have no disclosures.

Ethical approval The study protocol was approved by the Ethics Committee (Ethics number CER CHUM: 18.039 and 18.085-17.035) and conducted in accordance with the tenets of the Declaration of Helsinki. The need for informed patient consent was waived.

References

1. Horn L, Spigel DR, Vokes EE, Holgado E, Ready N, Steins M, et al. Nivolumab versus docetaxel in previously treated patients with advanced non–small-cell lung cancer: two-year outcomes from two randomized, open-label, phase III trials (CheckMate 017 and CheckMate 057). J Clin Oncol. 2017;35:3924–33. https://doi.org/10.1200/JCO.2017.74.3062.
2. Borghaei H, Paz-Ares L, Horn L, Spigel DR, Steins M, Ready NE, et al. Nivolumab versus docetaxel in advanced nonsquamous non–small-cell lung cancer. N Engl J Med. 2015;373:1627–39. https://doi.org/10.1056/NEJMoa1507643.
3. Brahmer J, Reckamp KL, Baas P, Crinò L, Eberhardt WEE, Poddubskaya E, et al. Nivolumab versus docetaxel in advanced squamous-cell non–small-cell lung cancer. N Engl J Med. 2015;373:123–35. https://doi.org/10.1056/NEJMoa1504627.
4. Rittmeyer A, Barlesi F, Waterkamp D, Park K, Ciardiello F, von Pawel J, et al. Atezolizumab versus docetaxel in patients with previously treated non-small-cell lung cancer (OAK): a phase 3, open-label, multicentre randomised controlled trial. Lancet. 2017;389:255–65. https://doi.org/10.1016/s0140-6736(16)32517-x.

5. Antonia SJ, Borghaei H, Ramalingam SS, Horn L, De Castro CJ, Pluzanski A, et al. Four-year survival with nivolumab in patients with previously treated advanced non-small-cell lung cancer: a pooled analysis. Lancet Oncol. 2019;20:1395–408. https://doi.org/10.1016/s1470-2045(19)30407-3.
6. Reck M, Rodriguez-Abreu D, Robinson AG, Hui R, Csoszi T, Fulop A, et al. Pembrolizumab versus chemotherapy for PD-L1-positive non-small-cell lung cancer. N Engl J Med. 2016;375:1823–33. https://doi.org/10.1056/NEJMoa1606774.
7. Paz-Ares L, Luft A, Vicente D, Tafreshi A, Gumus M, Mazieres J, et al. Pembrolizumab plus chemotherapy for squamous non-small-cell lung cancer. N Engl J Med. 2018;379:2040–51. https://doi.org/10.1056/NEJMoa1810865.
8. Elkrief A, Joubert P, Florescu M, Tehfe M, Blais N, Routy B. Therapeutic landscape of metastatic non-small-cell lung cancer in Canada in 2020. Curr Oncol. 2020;27:52–60. https://doi.org/10.3747/co.27.5953.
9. Herbst RS, Baas P, Kim DW, Felip E, Perez-Gracia JL, Han JY, et al. Pembrolizumab versus docetaxel for previously treated, PD-L1-positive, advanced non-small-cell lung cancer (KEYNOTE-010): a randomised controlled trial. Lancet. 2016;387:1540–50. https://doi.org/10.1016/s0140-6736(15)01281-7.
10. Doroshow DB, Sanmamed MF, Hastings K, Politi K, Rimm DL, Chen L, et al. Immunotherapy in non–small cell lung cancer: facts and hopes. Clin Cancer Res. 2019;25:4592–602. https://doi.org/10.1158/1078-0432.ccr-18-1538.
11. Socinski MA, Jotte RM, Cappuzzo F, Orlandi F, Stroyakovskiy D, Nogami N, et al. Atezolizumab for first-line treatment of metastatic nonsquamous NSCLC. N Engl J Med. 2018;378:2288–301. https://doi.org/10.1056/NEJMoa1716948.
12. Rizvi NA, Hellmann MD, Snyder A, Kvistborg P, Makarov V, Havel JJ, et al. Mutational landscape determines sensitivity to PD-1 blockade in non–small cell lung cancer. Science. 2015;348:124–8. https://doi.org/10.1126/science.aaa1348.
13. Routy B, Le Chatelier E, Derosa L, Duong CPM, Alou MT, Daillere R, et al. Gut microbiome influences efficacy of PD-1-based immunotherapy against epithelial tumors. Science. 2018;359:91–7. https://doi.org/10.1126/science.aan3706.
14. Chaput N, Lepage P, Coutzac C, Soularue E, Le Roux K, Monot C, et al. Baseline gut microbiota predicts clinical response and colitis in metastatic melanoma patients treated with ipilimumab. Ann Oncol. 2017;28:1368–79. https://doi.org/10.1093/annonc/mdx108.
15. Gopalakrishnan V, Spencer CN, Nezi L, Reuben A, Andrews MC, Karpinets TV, et al. Gut microbiome modulates response to anti-PD-1 immunotherapy in melanoma patients. Science. 2018;359:97–103. https://doi.org/10.1126/science.aan4236.
16. Matson V, Fessler J, Bao R, Chongsuwat T, Zha Y, Alegre ML, et al. The commensal microbiome is associated with anti-PD-1 efficacy in metastatic melanoma patients. Science. 2018;359:104–8. https://doi.org/10.1126/science.aao3290.
17. Jin Y, Dong H, Xia L, Yang Y, Zhu Y, Shen Y, et al. The diversity of gut microbiome is associated with favorable responses to anti-programmed death 1 immunotherapy in Chinese patients with NSCLC. J Thorac Oncol. 2019;14:1378–89. https://doi.org/10.1016/j.jtho.2019.04.007.
18. Elkrief A, Derosa L, Kroemer G, Zitvogel L, Routy B. The negative impact of antibiotics on outcomes in cancer patients treated with immunotherapy: a new independent prognostic factor? Ann Oncol. 2019;30:1572–9. https://doi.org/10.1093/annonc/mdz206.
19. Wilson BE, Routy B, Nagrial A, Chin VT. The effect of antibiotics on clinical outcomes in immune-checkpoint blockade: a systematic review and meta-analysis of observational studies. Cancer Immunol Immunother. 2020;69:343–54. https://doi.org/10.1007/s00262-019-02453-2.
20. Elkrief A, El Raichani L, Richard C, Messaoudene M, Belkaid W, Malo J, et al. Antibiotics are associated with decreased progression-free survival of advanced melanoma patients treated with immune checkpoint inhibitors. Oncoimmunology. 2019;8:e1568812. https://doi.org/10.1080/2162402X.2019.1568812.
21. Pinato DJ, Howlett S, Ottaviani D, Urus H, Patel A, Mineo T, et al. Association of prior antibiotic treatment with survival and response to immune checkpoint inhibitor therapy in patients with cancer. JAMA Oncol. 2019;5:1774–8. https://doi.org/10.1001/jamaoncol.2019.2785.
22. Derosa L, Routy B, Fidelle M, Iebba V, Alla L, Pasolli E, et al. Gut bacteria composition drives primary resistance to cancer immunotherapy in renal cell carcinoma patients. Eur Urol. 2020;78:195–206. https://doi.org/10.1016/j.eururo.2020.04.044.
23. Hakozaki T, Richard C, Elkrief A, Hosomi Y, Benlaïfaoui M, Mimpen I, et al. The gut microbiome associates with immune checkpoint inhibition outcomes in patients with advanced non–small cell lung cancer. Cancer Immunol Res. 2020; 8:1243–1250. https://doi.org/10.1158/2326-6066.CIR-20-0196.
24. Utzschneider KM, Kratz M, Damman CJ, Hullar M. Mechanisms linking the gut microbiome and glucose metabolism. J Clin Endocrinol Metab. 2016;101:1445–54. https://doi.org/10.1210/jc.2015-4251.
25. Boursi B, Werner TJ, Gholami S, Houshmand S, Mamtani R, Lewis JD, et al. Functional imaging of the interaction between gut microbiota and the human host: a proof-of-concept clinical study evaluating novel use for 18F-FDG PET-CT. PLoS One. 2018;13:e0192747. https://doi.org/10.1371/journal.pone.0192747.
26. Bybel B, Brunken RC, DiFilippo FP, Neumann DR, Wu G, Cerqueira MD. SPECT/CT imaging: clinical utility of an emerging technology. Radiographics. 2008;28:1097–113. https://doi.org/10.1148/rg.284075203.
27. Dore J, Ehrlich SD, Levenez F, Pelletier E, Alberti A, Bertrand L and IHMS Consortium (2015). IHMS_SOP 05 V1: Standard operating procedure forfecal samples preserved in stabilizing solution self-collection, laboratory analysis handled within 24 hours to 7 days (24 hours < x ≤ 7 days). International Human Microbiome Standards. 2015. http://www.microbiome-standards.org. Accessed March 5th, 2020.
28. Suau A, Bonnet R, Sutren M, Godon J-J, Gibson GR, Collins MD, et al. Direct analysis of genes encoding 16S rRNA from complex communities reveals many novel molecular species within the human gut. Appl Environ Microbiol. 1999;65:4799–807.
29. Visconti A, Martin TC, Falchi M. YAMP: a containerized workflow enabling reproducibility in metagenomics research. Gigascience. 2018;7:1–9. https://doi.org/10.1093/gigascience/giy072.
30. Segata N, Waldron L, Ballarini A, Narasimhan V, Jousson O, Huttenhower C. Metagenomic microbial community profiling using unique clade-specific marker genes. Nat Methods. 2012;9:811–4. https://doi.org/10.1038/nmeth.2066.
31. McMurdie PJ, Holmes S. phyloseq: an R package for reproducible interactive analysis and graphics of microbiome census data. PLoS One. 2013;8:e61217. https://doi.org/10.1371/journal.pone.0061217.
32. Bray JR, Curtis TJ. An ordination of upland forest communities of southern Wisconsin. Ecol Monogr. 1957;27:325–49. https://doi.org/10.2307/1942268.
33. Zhu C, Yu J. Nonmetric multidimensional scaling corrects for population structure in association mapping with different sample types. Genetics. 2009;182:875–88. https://doi.org/10.1534/genetics.108.098863.
34. Love MI, Huber W, Anders S. Moderated estimation of fold change and dispersion for RNA-seq data with DESeq2. Genome Biol. 2014;15:550. https://doi.org/10.1186/s13059-014-0550-8.
35. Eisenhauer EA, Therasse P, Bogaerts J, Schwartz LH, Sargent D, Ford R, et al. New response evaluation criteria in solid tumours:

revised RECIST guideline (version 1.1). Eur J Cancer. 2009;45:228–47. https://doi.org/10.1016/j.ejca.2008.10.026.
36. Kaplan EL, Meier P. Nonparametric estimation from incomplete observations. J Am Stat Assoc. 1958;53:457–81. https://doi.org/10.1080/01621459.1958.10501452.
37. Mantel N. Evaluation of survival data and two new rank order statistics arising in its consideration. Cancer Chemother Rep. 1966;50:163–70.
38. Lozupone CA, Stombaugh JI, Gordon JI, Jansson JK, Knight R. Diversity, stability and resilience of the human gut microbiota. Nature. 2012;489:220–30. https://doi.org/10.1038/nature11550.
39. Turnbaugh PJ, Ley RE, Mahowald MA, Magrini V, Mardis ER, Gordon JI. An obesity-associated gut microbiome with increased capacity for energy harvest. Nature. 2006;444:1027–31. https://doi.org/10.1038/nature05414.
40. Blander JM, Longman RS, Iliev ID, Sonnenberg GF, Artis D. Regulation of inflammation by microbiota interactions with the host. Nat Immunol. 2017;18:851–60. https://doi.org/10.1038/ni.3780.
41. Boursi B, Werner TJ, Gholami S, Margalit O, Baruch E, Markel G, et al. Physiologic colonic fluorine-18-fluorodeoxyglucose uptake may predict response to immunotherapy in patients with metastatic melanoma. Melanoma Res. 2019;29:318–21. https://doi.org/10.1097/cmr.0000000000000566.
42. Vetizou M, Pitt JM, Daillere R, Lepage P, Waldschmitt N, Flament C, et al. Anticancer immunotherapy by CTLA-4 blockade relies on the gut microbiota. Science. 2015;350:1079–84. https://doi.org/10.1126/science.aad1329.
43. Zheng Y, Wang T, Tu X, Huang Y, Zhang H, Tan D, et al. Gut microbiome affects the response to anti-PD-1 immunotherapy in patients with hepatocellular carcinoma. J Immunother Cancer. 2019;7:193. https://doi.org/10.1186/s40425-019-0650-9.